2.3. Data collection and processing

The recording and analysis procedures were the same as those described elsewhere (Kasai et al., 2001, 2002, 2003). Magnetic fields were recorded in a magnetically shielded room (NKK Plant Engineering Co., Japan) with a 122 channel magnetometer (Neuromag Ltd., Finland; Knuutila et al., 1993). This whole-head magnetometer consists of 61 dual-sensor units, each with two orthogonal planar gradiometers for recording maximal signals directly above the source (Hämäläinen et al., 1993). The subjects sat on a chair with their head inside the helmet-shaped magnetometer. The position of the magnetometer with respect to the head was determined at the beginning of the task under each condition by recording the magnetic fields produced by currents fed into 3 indicator coils at predetermined locations on the scalp. The locations of these coils in relation to the preauricular points and nasion were determined with an Isotrak 3D-digitizer (Polhemus TM, USA) before the start of the experiment. One electrode was placed at the outer canthus and another one below the left eye to monitor eye movements.

MEG epochs were averaged separately for standard and deviant stimuli online. The duration of the averaging period was 512 ms, including a 64 ms prestimulus baseline. The recording bandpass was 0.03–100 Hz, with a sampling rate of 500 Hz. The first 10 stimuli were automatically excluded from averaging. Epochs coinciding with electrooculogram movement or MEG exceeding 150 μV or 3000 fT/cm were also excluded from averaging. Each condition lasted until 100 deviant stimuli without contamination of artifacts were acquired. Averaged responses were digitally filtered with a bandpass of 1–30 Hz.

2.4. MMF measurement

For each subject in each condition, equivalent current dipoles (ECDs) for MMF were calculated primarily according to the method used by Alho et al. (1998b). Briefly, the MMF was determined from the difference curves obtained by subtracting the response to standard stimuli from that to deviant stimuli. ECDs were then determined using a least-squares fit at 2 ms intervals from 100 to 250 ms. The calculation was performed separately for each hemisphere (a subset of 44 channels over the temporal brain areas), utilizing a spherical head model in which the center of the model sphere was placed 45 mm above the origin of the coordinate system (Alho et al., 1998b). ECDs with a maximal goodness of fit (GOF) $\geq 60\%$ were included in the analysis. In this procedure, we reduced the number of channels to 28–43 when the dipole was not calculated or a certain channel had a considerable number of artifacts. The mean GOFs under the 3 conditions and in the two hemispheres ranged from 78.3 to 85.7% for the autism group and 72.5 to 85.7% for the control group, and did not differ between groups for any condition or hemisphere (Mann–Whitney's U test, $Ps > 0.23$).

The subjects for whom ECDs were not reliably calculated for at least one hemisphere were 6/19 for the control group and 9/9 for the autism group. In the control group, visual inspection of the signals for these cases indicated that MMF was strongly lateralized to one hemisphere, possibly resulting in the failure to calculate ECDs in the other hemisphere. In the autism individuals, there were no gross artifacts or noises superimposed on averaged response curves that would account for the failure to calculate ECDs. In theory, the ECD is stronger when neuronal activities are synchronized and regionalized (Kasai et al., 2002, 2003). Thus, an alternative explanation for the failure to calculate ECDs may be that some individuals with autism had deficits in the synchronization and regionalization of the neuronal population involved in MMF generation.

To utilize the data of all the subjects in the statistical analyses, the magnitude of MMF responses was reassessed by applying global field power (GFP; Lehmann and Skrandies, 1980) to the analysis of MEG data (magnetic counterpart of GFP [mGFP]; Kasai et al., 2001, 2002, 2003; Kreitschmann-Andermahr et al., 1999; Rosberg et al., 2000). First, for each subject, the mGFP was calculated separately for each condition and hemisphere using the same 44 channels as those used in the dipole analysis. In this procedure, the number of channels was reduced to 28–43 when a certain channel had a considerable number of artifacts. The peak latency of MMF for each subject was determined based on the individual mGFP curve as a function of time. Second, the grand mean mGFP curves were plotted. The MMF power for each subject was then determined as the mean mGFP within a 100 ms window around the peak latency of the grand mean mGFP. This 100 ms window was chosen because it was within the length of clear evocation of MMF (Fig. 1). Our previous studies have shown the mGFP power/latency to be a good substitute for ECD strength/latency (Kasai et al., 2001, 2002, 2003).

2.5. Statistical analysis

Group differences in dipole strength and location were tested using Mann–Whitney U test. The t tests were performed for the group comparison of MMF power or latency for each condition and hemisphere. Since there were 12 multiple comparisons, the level for significance was set at $P = 0.0042$ (Bonferroni correction). Moreover, since there was unequal sample size and, in two conditions unequal variance (Levene's test for equality of variance; tone-duration, left hemisphere: $P = 0.02$; phoneme-duration, left hemisphere: $P = 0.008$; other conditions: $P > 0.28$) between the groups, we also performed non-parametric Mann–Whitney U test for confirmation purpose. Spearman's rho was calculated for correlations between MMF indices and total CARS scores in the autism group. Additionally,

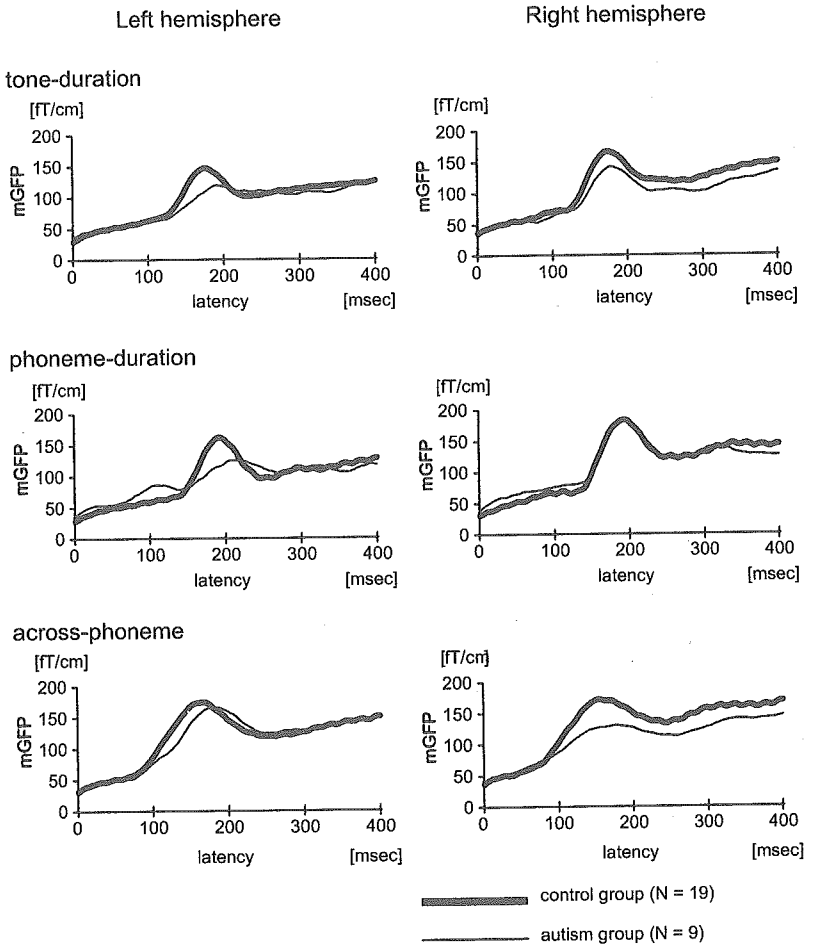

Fig. 1. Grand mean magnetic counterpart of global field power (mGFP) waveforms under the tone-duration (top), the phoneme-duration (middle), and the across-phoneme (bottom) change condition for each hemisphere. Thick lines are for the control group and thin lines for the autism group.

Spearman's correlations between MMF indices and age (for each of both groups), IQ scores (autism group only) or neuroleptics and anticholinergic dose (autism group only) were calculated to test for potential confounding status of these indices.

3. Results

3.1. Dipole analysis

An example of dipole locations superimposed on a subject's magnetic resonance imaging is shown in Fig. 2. For this subject, MMF for each condition was located in the vicinity of the posterior superior temporal gyrus in each hemisphere, coinciding with previous reports on source localization of MMF in response to pure tones (Alho et al., 1998b) or speech sounds (Alho et al., 1998a).

Group differences in dipole strengths or locations were not statistically significant for any condition or hemisphere after Bonferroni correction (the level of significance was $P=0.002$; 24 comparisons) (Table 2).

3.2. MMF power and latency

The t tests showed that the autism group was associated with significantly delayed latency of MMF under the across-phoneme condition in the left hemisphere ($t[26]=3.11$, $P=0.004$) (Table 3). Additionally, these results were confirmed by Mann–Whitney U test which showed a significance in the left hemisphere of across-phoneme condition ($Z=-2.46$, $P=0.014$), while other conditions/hemisphere did not reach significance ($P>0.07$).

3.3. Correlational analyses

Autism individuals' MMF latency in the left hemisphere under the across-phoneme condition showed a significant positive correlation with scores for CARS (rho=0.672, $N=9$, $P=0.047$). Importantly, MMF latency in the left hemisphere under the across-phoneme condition in

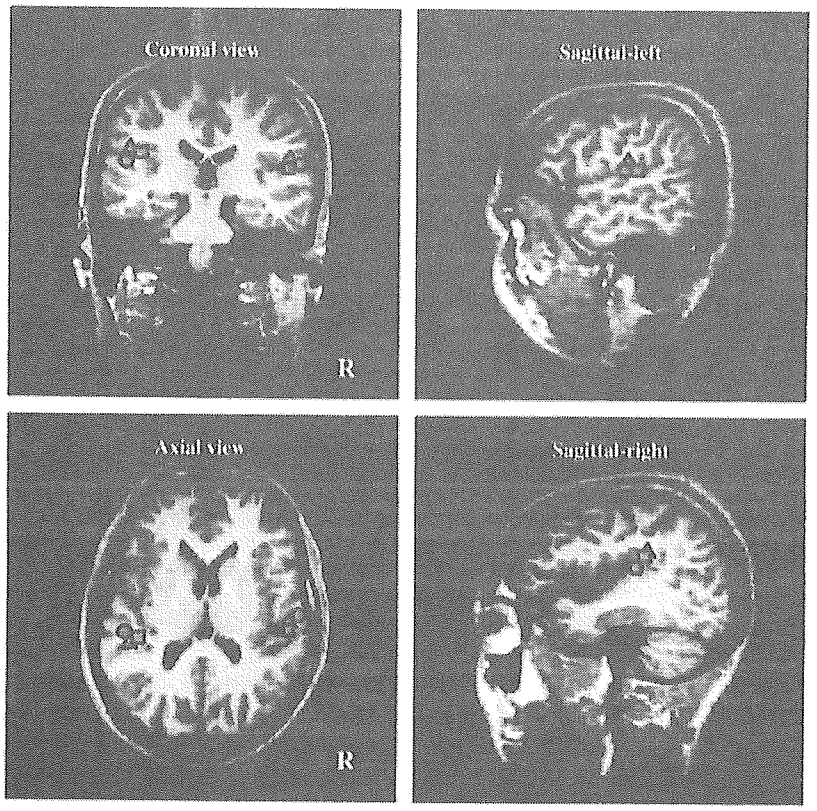

Fig. 2. Locations of equivalent current dipoles (ECDs) under each condition in each hemisphere of a control subject superimposed on a magnetic resonance imaging slice of this subject. Circle: ECD location of MMF under tone-duration condition; triangle: that under phoneme-duration condition; and square: that under across-phoneme condition.

the autism group was not significantly correlated with age (rho = −0.126, $N=9$, $P=0.75$), IQ (rho = −0.285, $N=9$, $P=0.46$), or dose of medication (neuroleptics: rho = 0.173, $N=9$, $P=0.66$; anticholinergic drugs: rho = 0.419, $N=9$, $P=0.26$).

Additional significant results were as follows: control subjects' MMF power under the across-phoneme condition showed a significant negative correlation with age (left hemisphere: rho = −0.552, $N=19$, $P=0.014$; right hemisphere: rho = −0.693, $N=19$, $P=0.001$); autism individuals' MMF latency in the right hemisphere under the phoneme-duration condition showed a significant negative correlation with IQ (rho = −0.689, $N=9$, $P=0.04$); patient's MMF latency in the left hemisphere under the phoneme-duration condition showed a significant negative correlation with neuroleptic dose (rho = −0.676, $P=0.046$) and anticholinergic drugs (rho = −0.698, $P=0.037$).

4. Discussion

The present findings represent the first physiological evidence, derived from whole-head MEG, of delayed automatic processing of change in speech sounds predominantly in the left temporal area in adults with autism. Moreover, to our knowledge, this is the first study that linked MMN/MMF abnormalities to clinical severity in autism. This study suggests that language-related dysfunction in autism may be present at the early stage of auditory processing of relatively simple stimuli such as phonemes, and not just at stages involving higher-order semantic processes. In this study, the autism group showed neither abnormal power nor lateralization for any type of MMF, while MMF latency was prolonged in the left hemisphere during across-category change detection of vowels. Although conclusions must be speculative, it may be that adults with autism have difficulties in rapid evaluation of change in speech sounds, particularly that mediated in the left auditory cortex. These results are also consonant with PET (Boddaert et al., 2003; Zilbovicius et al., 2000) and single photon emission computed tomography (Hashimoto et al., 2000; Ohnishi et al., 2000) studies that report temporal lobe hypoperfusion in autism.

Additionally, the results of the present study indicate that adults with autism did not show marked deficits in duration MMF in response to tones and vowels, although this discussion should be regarded as tentative since there appeared to be a statistically non-significant difference in the left hemisphere. Since no previous study has measured duration MMN/MMF in autism, future studies should assess

Table 2
Equivalent current dipole strength and location in control subjects and autism patients

	Control group			Autism group			Group comparison[a]	
	N	Mean	SD	*N*	Mean	SD	*Z*	*P*
ECD strength (nAm)								
Pure (L)	17	22.2	11.3	5	20.5	9.1	−0.39	0.70
Pure (R)	16	27.3	11.9	8	30.9	6.9	−0.92	0.36
a/a (L)	17	28.3	16.4	3	27.7	26.5	−0.58	0.56
a/a (R)	19	32.8	19.4	7	34.4	9.7	−0.84	0.40
a/o (L)	19	29.0	9.9	7	28.4	15.9	−0.35	0.73
a/o (R)	18	27.9	11.8	5	33.2	16.2	−0.82	0.41
ECD location[b] (mm)								
x-axis								
Pure (L)	17	−53.5	7.7	5	−49.1	6.8	−1.06	0.29
Pure (R)	16	52.7	10.8	8	49.7	8.5	−0.73	0.46
a/a (L)	17	−55.0	8.5	3	−54.5	11.2	−0.21	0.83
a/a (R)	19	51.3	10.6	7	53.4	9.2	−0.26	0.79
a/o (L)	19	−54.0	8.8	7	−49.4	10.9	−0.90	0.37
a/o (R)	18	53.5	6.4	5	56.3	5.7	−0.89	0.37
y-axis								
Pure (L)	17	6.2	8.5	5	6.6	6.5	−0.04	0.97
Pure (R)	16	11.7	8.1	8	4.4	7.5	−2.08	0.04
a/a (L)	17	8.7	8.0	3	−0.9	6.8	−1.85	0.06
a/a (R)	19	13.1	11.6	7	11.3	8.2	−0.20	0.84
a/o (L)	19	7.7	7.6	7	4.1	8.5	−0.84	0.40
a/o (R)	18	13.5	12.2	5	6.4	5.8	−1.53	0.13
z-axis								
Pure (L)	17	65.5	10.5	5	66.7	11.2	−0.04	0.97
Pure (R)	16	66.3	9.4	8	61.8	11.4	−1.13	0.26
a/a (L)	17	60.5	9.8	3	61.4	8.0	−0.16	0.87
a/a (R)	19	65.4	8.7	7	69.3	7.2	−1.19	0.24
a/o (L)	19	64.1	10.9	7	66.1	10.9	−0.14	0.89
a/o (R)	18	64.7	11.7	5	57.8	16.8	−1.04	0.30

ECD, equivalent current dipole; pure, tone-duration condition; a/a, phoneme-duration condition; a/o, across-phoneme condition; L, left hemisphere; R, right hemisphere.

[a] Mann–Whitney *U* test. The level of significance was $P=0.002$ (Bonferroni correction; 24 comparisons).

[b] The coordinate system was defined so that the *x*-axis passes through the preauricular points, with the positive *x*-axis pointing to the right. The *y*-axis passes the nasion, pointing anteriorly, and the *z*-axis points upwards.

Table 3
Global field power and latency of the magnetic mismatch field

	Autism group ($N=9$)		Control group ($N=19$)		Effect size	*T* test (df = 26)	
	Mean	SD	Mean	SD		*T* value	*P* value
Global field power (fT/cm)							
Tone-duration (left)	106	26	119	33	0.39	−0.98	0.34
Tone-duration (right)	117	34	134	40	0.43	−1.11	0.28
Phoneme-duration (left)	115	36	126	40	0.28	−0.67	0.51
Phoneme-duration (right)	147	32	148	34	0.03	−0.06	0.95
Across-phoneme (left)	149	65	153	47	0.09	−0.2	0.84
Across-phoneme (right)	124	47	154	45	0.67	−1.63	0.11
Peak latency (ms)							
Tone-duration (left)	194	30	177	16	1.06	2.02	0.054
Tone-duration (right)	181	11	175	12	0.50	1.24	0.23
Phoneme-duration (left)	194	36	189	9	0.56	0.59	0.56
Phoneme-duration (right)	193	12	193	14	0.00	0.11	0.91
Across-phoneme (left)	186	23	161	19	1.32	3.11	0.004[a]
Across-phoneme (right)	172	35	162	29	0.34	0.74	0.46

df, degree of freedom.

[a] Significantly delayed in the autism group. Statistically significance level was $P=0.0042$ (Bonferroni correction for 12 comparisons).

not only frequency MMN/MMF but also duration MMN/MMF to confirm our findings. Moreover, some electrophysiological studies have suggested abnormalities in temporal lobe auditory processing as reflected by N1 component in response to tones (e.g. Bruneau et al., 1999; Lincoln et al., 1995), although a direct comparison between N1 and MMN components should be cautioned as they reflect different aspects of sound processing. Some hemodynamic studies have also reported temporal lobe hypoperfusion in the resting state, which indicate overall dysfunction in the auditory cortex (Hashimoto et al., 2000; Ohnishi et al., 2000; Zilbovicius et al., 2000). Our design did not test the hypothesis that the auditory cortex dysfunction in autism is speech-sound specific, which should be tested in future studies.

The present study found a group difference in MMF latency, but not in MMF power. Previous findings from MMN/MMF studies in autism have been mixed. Three studies reported preserved MMN amplitude (Čeponienė et al., 2003; Gomot et al., 2002; Kemner et al., 1995), two studies reported reduced MMN/MMF amplitude/power (Seri et al., 1999; Tecchio et al., 2003), and one study reported enhanced MMN in autism (Ferri et al., 2003). As for latency, only Seri et al. (1999) reported prolonged latency of MMN in response to tones, whereas Gomot et al. (2002) reported shorter latency of tonal MMN in children with autism. The interpretation of Seri et al. study should be done with caution, since they tested subjects with tuberous sclerosis, which is not a typical case of autism. Gomot et al. explained their shorter tone-MMN latency by an overlap with an early P3a component. Moreover, Gomot et al. used frequency changes in pure tones, while our study used duration changes in pure tones and vowels and phoneme changes in vowels. This difference in the type of stimuli may partly explain the difference in results between the two studies. Two other studies reported intact MMN latency (Čeponienė et al., 2003; Ferri et al., 2003), and the remaining two provided no information on latency findings (Kemner et al., 1995; Tecchio et al., 2003). Čeponienė et al. (2003) found no differences between autistic and control children in MMN elicited by speech sound changes. The subjects of our study were adults, while the subjects of theirs were children. Delayed latency of MMN in response to speech sounds may be more evident in adults with autism, possibly due to a lack of normal development of specialization (or functional plasticity) for processing of speech sounds.

To our knowledge, the present study is the first to demonstrate a significant association between mismatch abnormalities and clinical symptoms in autism. However, due to a small sample size and a restricted range of CARS scores in our sample, the results should be regarded as tentative. Future studies should clarify how MMN/MMF abnormalities are related to specific cognitive profiles and social and communication problems, in individuals with autism.

Some other methodological issues in the current study need to be commented upon. First, a follow-up experiment employing children with autism should be conducted to generalize our findings. Secondly, the subject group was not restricted to high-functioning autism individuals to match IQ to healthy subjects, nor was there an IQ-matched (intellectually disabled) control group. However, since MMF indices were not significantly correlated with IQ, employing low-functioning subjects may not have produced marked confounds in the interpretation of our findings. However, since previous studies have shown lower amplitude of phonetic MMN in subjects with learning disabilities (Bradlow et al., 1999) and in those with intellectual disabilities (Kaga et al., 1999), future studies should employ individuals with learning and intellectual disabilities as a control group to clarify whether the present findings are specific to autism. Thirdly, although we found a significant negative correlation between dose of medication and some of the MMF latency indices, these correlations were not in a predicted direction. These results should not be considered to be definitive, however, since (1) the sample size is small and (2) uncorrected *P*s of 0.046 and 0.037 may not remain significant after a correction for multiple statistical comparisons.

In conclusion, this study, using a whole-head MEG, provides physiological evidence for delayed processing of change in speech sounds in the left auditory cortex in adults with autism. Our next goal will be to elucidate the relationship of this physiological abnormality of speech sounds at the basic level with higher-order communication deficits in autism.

Acknowledgements

This work was supported in part by a Grant-in-Aid for Scientific Research (C12670928 to Drs Kasai, Iwanami, and Itoh) from the Ministry of Education, Culture, Sports, Science and Technology, Japan. The authors gratefully thank Dr Mark Rogers for his helpful comments and English editing on the manuscript.

References

Alain C, Woods DL, Knight RT. A distributed cortical network for auditory sensory memory in humans. Brain Res 1998;812:22–37.

Alho K, Woods DL, Knight RT, Näätänen R. Lesions of frontal cortex diminish the auditory mismatch negativity. Electroencephalogr Clin Neurophysiol 1994;91:353–62.

Alho K, Connolly JF, Cheour M, Lehtokoski A, Huotilainen M, Virtanen J, Aulanko R, Ilmoniemi RJ. Hemispheric lateralization in preattentive processing of speech sounds. Neurosci Lett 1998a;258: 9–12.

Alho K, Winkler I, Escera C, Huotilainen M, Virtanen J, Jääskeläinen IP, Pekkonen E, Ilmoniemi RJ. Processing of novel sounds and frequency

changes in the human auditory cortex: magnetoencephalographic recordings. Psychophysiology 1998b;35:211–24.

American Psychiatric Association. Diagnostic and statistical manual of mental disorders. 4th ed. Washington DC: American Psychiatric Press; 1994.

Boddaert N, Belin P, Chabane N, Poline J-B, Barthélémy C, Mouren-Simeoni M-C, Brunelle F, Samson Y, Zilbovicius M. Perception of complex sounds: abnormal pattern of cortical activation in autism. Am J Psychiatry 2003;160:2057–60.

Bradlow AR, Kraus N, Nicol TG, McGee TJ, Cunningham J, Zecker SG, Carrell TD. Effects of lengthened formant transition duration on discrimination and neural representation of synthetic CV syllables by normal and learning-disabled children. J Acoust Soc Am 1999;106: 2086–96.

Bruneau N, Roux S, Adrien JL, Barthélémy C. Auditory associative cortex dysfunction in children with autism: evidence from late auditory evoked potentials (N1 wave–T complex). Clin Neurophysiol 1999;110: 1927–34.

Čeponienė R, Lepistö T, Shestakova A, Vanhala R, Alku P, Näätänen R, Yaguchi K. Speech-sound-selective auditory impairment in children with autism: they can perceive but do not attend. Proc Natl Acad Sci USA 2003;100:5567–72.

Dawson G, Meltzoff AN, Osterling J, Rinaldi J, Brown E. Children with autism fail to orient to naturally occurring social stimuli. J Autism Dev Disord 1998;28:479–85.

Ferri R, Elia M, Agarwal N, Lanuzza B, Musumeci SA, Pennisi G. The mismatch negativity and the P3a components of the auditory event-related potentials in autistic low-functioning subjects. Clin Neurophysiol 2003;114:1671–80.

Giard MH, Perrin F, Pernier J, Bouchet P. Brain generators implicated in the processing of auditory stimulus deviance: a topographic event-related potential study. Psychophysiology 1990;27:627–40.

Gomot M, Giard M-H, Adrien J-L, Barthelemy C, Bruneau N. Hypersensitivity to acoustic change in children with autism: electrophysiological evidence of left frontal cortex dysfunctioning. Psychophysilogy 2002; 39:577–84.

Hämäläinen M, Hari R, Ilmoniemi R, Knuutila J, Lounasmaa OV. Magnetoencephalography: theory, instrumentation, and applications to noninvasive studies of the working human brain. Rev Mod Phys 1993;65:413–97.

Hari R, Hämäläinen M, Ilmoniemi R, Kaukoranta E, Reinilainen K, Salminen J, Alho K, Näätänen R, Sams M. Responses of the primary auditory cortex to pitch changes in a sequence of tone pips: neuromagnetic recordings in man. Neurosci Lett 1984;50: 127–32.

Hashimoto T, Sasaki M, Fukumizu M, Hanaoka S, Sugai K, Matsuda H. Single-photon emission computed tomography of the brain in autism: effect of the developmental level. Pediatr Neurol 2000;23:416–20.

Inagaki A, Inada T, Fujii Y, Yagi G. Dose equivalence of neuroleptics. In: Inagaki A, Inada T, Fujii Y, Yagi G, Yoshio T, Nakamura H, Yamauchi T, editors. Dose equivalence of psychotropic drugs. Tokyo: Seiwa Publishers; 1999. p. 11–60 (in Japanese).

Inagaki A, Inada T, Fujii Y, Yagi G. Dose equivalence of neuroleptics. In: Inagaki A, Inada T, Fujii Y, Yagi G, Yoshio T, Nakamura H, Yamauchi T, editors. Dose equivalence of psychotropic drugs. Tokyo: Seiwa Publishers; 1999. p. 61–76 (in Japanese).

Kaga M, Inagaki M, Uno A. Auditory verbal and non-verbal mismatch negativity (MMN) in patients with severe motor and intellectual disabilities. Electroencephalogr Clin Neurophysiol Suppl. 1999;49: 194–8.

Kasai K, Nakagome K, Itoh K, Koshida I, Hata A, Iwanami A, Fukuda M, Hiramatsu K-I, Kato N. Multiple generators in the auditory automatic discrimination process in humans. NeuroReport 1999;10:2267–71.

Kasai K, Yamada H, Kamio S, Nakagome K, Iwanami A, Fukuda M, Itoh K, Koshida I, Yumoto M, Iramina K, Kato N, Ueno S. Brain lateralization for mismatch response to across- and within-category change of vowels. NeuroReport 2001;12:2467–71.

Kasai K, Yamada H, Kamio S, Nakagome K, Iwanami A, Fukuda M, Yumoto M, Itoh K, Koshida I, Abe O, Kato N. Do high or low doses of anxiolytics and hypnotics affect mismatch negativity in schizophrenic subjects? An EEG and MEG study Clin Neurophysiol 2002;113: 141–50.

Kasai K, Yamada H, Kamio S, Nakagome K, Iwanami A, Fukuda M, Yumoto M, Itoh K, Koshida I, Abe O, Kato N. Neuromagnetic correlates of impaired automatic categorical perception of speech sounds in schizophrenia. Schizophr Res 2003;59:159–72.

Kemner C, Verbaten MN, Cuperus JM, Camfferman G, van Engeland H. Auditory event-related brain potentials in autistic children and three different control groups. Biol Psychiatry 1995;38:150–65.

Knuutila JET, Ahonen A, Hämäläinen MS, Kajola MI, Laine PP, Lounasmaa OV, Parkkonen LT, Simola JT, Tesche CD. A 122-channel whole-cortex SQUID system for measuring brain's magnetic field. IEEE Trans Magn 1993;29:3315–20.

Koyama S, Gunji A, Yabe H, Oiwa S, Akahane-Yamada R, Kakigi R, Näätänen R. Hemispheric lateralization in an analysis of speech sounds: left hemispheric dominance replicated in Japanese subjects. Brain Res Cogn Brain Res 2000;10:119–24.

Kraus N. Speech sound representation, perception, and plasticity: a neurophysiological perspective. Audiol Neurootol 1998;3:168–82.

Kreitschmann-Andermahr I, Rosburg T, Meier T, Volz HP, Nowak H, Sauer H. Impaired sensory processing in male patients with schizophrenia: a magnetoencephalographic study of auditory mismatch detection. Schizophr Res 1999;35:121–9.

Kurita H, Miyake Y, Katsuno K. Reliability and validity of the Childhood Autism Rating Scale—Tokyo version (CARS-TV). J Autism Dev Disord 1989;19:389–96.

Lehmann D, Skrandies W. Reference-free identification of components of checkboard-evoked multichannel potential fields. Electroencephalogr Clin Neurophysiol 1980;48:609–21.

Liasis A, Towell A, Alho K, Boyd S. Intracranial identification of an electric frontal-cortex response to auditory stimulus change: a case study. Brain Res Cogn Brain Res 2001;11:27–233.

Lincoln AJ, Courchesne E, Harms L, Allen M. Sensory modulation of auditory stimuli in children with autism and receptive developmental language disorder: event-related brain potential evidence. J Autism Dev Disord 1995;25:521–39.

Mesibov GB, Schopler E, Schaffer B, Michal N. Use of the childhood autism rating scale with autistic adolescents and adults. J Am Acad Child Adolesc Psychiatry 1989;28:538–41.

Näätänen R. The mismatch negativity (MMN). In: Attention and brain function. Hillsdale: Lawrence Erlbaum Associates; 1992: p. 136–200.

Näätänen R. The perception of speech sounds by the human brain as reflected by the mismatch negativity (MMN) and its magnetic equivalent (MMNm). Psychophysiology 2001;38:1–21.

Näätänen R, Gaillard AWK, Mäntysalo S. Early selective-attention effect on evoked potential reinterpreted. Acta Psychol 1978;42: 313–29.

Näätänen R, Lehtokoski A, Lennes M, Cheour M, Huotilainen M, Iivonen A, Vainio M, Alku P, Ilmoniemi RJ, Luuk A, Allik J, Sinkkonen J, Alho K. Language-specific phoneme representations revealed by electric and magnetic brain responses. Nature 1997;385:432–4.

Ohnishi T, Matsuda H, Hashimoto T, Kunihiro T, Nishikawa M, Uema T, Sasaki M. Abnormal regional cerebral blood flow in childhood autism. Brain 2000;123:1838–44.

Oldfield RC. The assessment and analysis of handedness: The Edinburgh inventory. Neuropsychologia 1971;9:97–113.

Rapin I. Autism. N Engl J Med 1997;337:97–104.

Rinne T, Alho K, Alku P, Holi M, Sinkkonen J, Virtanen J, Bertrand O, Näätänen R. Analysis of speech sounds is left-hemisphere predominance at 100–150 ms after sound onset. NeuroReport 1999;10:1113–7.

Rosburg T, Kreitschmann-Andermahr I, Nowak H, Sauer H. Habituation of the auditory evoked field component N100m in male patients with schizophrenia. J Psychiatr Res 2000;34:245–54.

Seri S, Cerquiglini A, Pisani F, Curatolo P. Autism in tuberous screlosis: evoked potential evidence for a deficit in auditory sensory processing. Clin Neurophysiol 1999;110:1825–30.

Shinagawa F, Kobayashi S, Fujita K, Maekawa H. Japanese Wechsler Adult Intelligence Scale-Revised. Tokyo: Nihon-bunka-kagakusha publishers; 1990 (in Japanese).

Swettenham J, Baron-Cohen S, Charman T, Cox A, Baird G, Drew A, Rees L, Wheelwright S. The frequency and distribution of spontaneous attention shifts between social and nonsocial stimuli in autistic, typically developing, and nonautistic developmentally delayed infants. J Child Psychol Psychiatry 1998;39:747–53.

Tanaka Institute for Education. Tanaka–Binet Intelligence Scale. Tokyo: Taken Publishers; 1987 (in Japanese).

Tecchio F, Benassi F, Zappasodi F, Gialloreti LE, Palermo M, Seri S, Rossini PM. Auditory sensory processing in autism: a magnetoencephalographic study. Biol Psychiatry 2003;54:647–54.

Tervaniemi M, Medvedev SV, Alho K, Pakhomov SV, Roudas MS, van Zuijen TL, Näätänen R. Lateralized automatic auditory processing of phonetic versus musical information: a PET study. Hum Brain Mapp 2000;10:74–9.

Umbricht D, Schmid L, Koller R, Vollenweider FX, Hell D, Javitt DC. Ketamine-induced deficits in auditory and visual context-dependent processing in healthy volunteers: implications for models of cognitive deficits in schizophrenia. Arch Gen Psychiatry 2000;57:1139–47.

Wechsler D. Wechsler Adult Intelligence Scale-Revised. New York: Harcourt Brace Jovanovich Inc; 1981.

Zilbovicius M, Boddaert N, Belin P, Poline J-B, Remy P, Mangin J-F, Thivard L, Barthélémy C, Samson Y. Temporal lobe dysfunction in childhood autism: a PET study. Am J Psychiatry 2000;157:1988–93.

ELSEVIER

NeuroImage

www.elsevier.com/locate/ynimg
NeuroImage 25 (2005) 43–50

Association between lower P300 amplitude and smaller anterior cingulate cortex volume in patients with posttraumatic stress disorder: a study of victims of Tokyo subway sarin attack

Tsuyoshi Araki,[a,*] Kiyoto Kasai,[a,*] Hidenori Yamasue,[a] Nobumasa Kato,[a] Noriko Kudo,[a,b] Toshiyuki Ohtani,[a] Kazuyuki Nakagome,[c] Kenji Kirihara[d], Haruyasu Yamada,[e] Osamu Abe,[e] and Akira Iwanami[f]

[a]*Department of Neuropsychiatry, Graduate School of Medicine, University of Tokyo, 7-3-1 Hongo, Bunkyo-ku, Tokyo 113-8655, Japan (the place where the work was carried out)*
[b]*Department of Cognitive and Information Sciences, Graduate School of Humanities, Chiba University, Chiba, Japan*
[c]*Department of Psychiatry, Showa University School of Medicine, Tokyo, Japan*
[d]*Department of Psychiatry, National Center Hospital for Mental, Nervous, and Muscular Disorders, National Center of Neurology and Psychiatry (NCNP), Tokyo, Japan*
[e]*Department of Radiology, Graduate School of Medicine, University of Tokyo, Tokyo, Japan*
[f]*Department of Medical Technology, Aino University, Osaka, Japan*

Received 2 March 2004; revised 10 August 2004; accepted 30 November 2004
Available online 29 December 2004

Previous investigations of auditory P300 event-related potentials have provided electrophysiological evidence for attentional problems in patients with posttraumatic stress disorder (PTSD). The present study sought to evaluate the relationship between P300 deficits and underlying brain morphological abnormalities in never-treated, comorbidity-free patients with PTSD following the Tokyo subway sarin attack. Out of 47 victims recruited, 8 victims with PTSD and 13 victims without PTSD were identified. Correlational analyses were performed between auditory P300 amplitude at Pz electrode site elicited in an oddball task and anterior cingulate gray matter volume that was shown to be reduced in our previous study using voxel-based morphometry on magnetic resonance imaging. Victims with PTSD showed significantly lower amplitudes of P300 compared with victims without PTSD, and the lower P300 amplitudes at Pz were significantly associated with higher avoidance/numbing scores in the PTSD group. Furthermore, in the PTSD group only, the P300 amplitudes showed a trend toward significant positive correlation with voxel densities of the anterior cingulate cortex gray matter. These results provide the first evidence that electrophysiological deficits of controlled attention observed in patients with PTSD may be linked to underlying brain morphological abnormalities.

Keywords: Posttraumatic stress disorder; Event-related potentials (ERPs); P300; Magnetic resonance imaging (MRI); Anterior cingulate cortex

Introduction

Posttraumatic stress disorder (PTSD) is a psychiatric condition associated with a constellation of disabling behavioral and emotional symptoms (e.g., nightmares, flashbacks, and intrusive recollections of traumatic events) which occur in a proportion of individuals exposed to severe psychological trauma, such as combat, sexual abuse, natural disasters, and terrorism. In addition, PTSD is associated with cognitive deficits, specifically impaired attention, such as difficulty in concentrating and sustaining attention on target tasks. These attentional problems in PTSD have been evaluated using auditory P300 event-related potentials (ERPs). The P300 has been shown to represent one's ability to allocate attentional resources and to update environmental context (Donchin and Coles, 1988; Picton, 1992; Polich and Kok, 1995). When the subject is instructed to attend to a target sound, the P300 is maximal at parietal sites and is often called P3b. Thus, the auditory P3b reflects an executive ability to sustain attention to target stimuli (Ford et al., 1976) and/or a capacity to allocate attention (Comerchero and Polich, 1999; Katayama and Polich, 1998).

Reviewing previous literature on auditory P3b in PTSD, McFarlane et al. (1993) employed a 3-tone oddball task with patients with PTSD due to a variety of traumatic events and found P3b reductions in response to rare target stimuli. These findings have been replicated in both classical oddball (2-tone) and 3-tone oddball studies (Charles et al., 1995; Felmingham et al., 2002; Metzger et al., 1997a,b). In contrast, Kimble et al. (2000) and Neylan et al. (2003) did not find P3b reduction in combat veterans

* Corresponding authors. Fax: +81 3 5800 6894.
E-mail addresses: taraki-tky@umin.ac.jp (T. Araki), kasaik-tky@umin.ac.jp (K. Kasai).
Available online on ScienceDirect (www.sciencedirect.com).

1053-8119/$ - see front matter © 2005 Elsevier Inc. All rights reserved.
doi:10.1016/j.neuroimage.2004.11.039

with PTSD. Metzger et al. (2002) found larger target P3b in female Vietnam nurse veterans with PTSD.

With regard to the relationship between these P300 abnormalities and clinical symptoms, however, there is little consensus in the previous literature; only one group (Felmingham et al., 2002) found an association with specific symptoms of PTSD. Felmingham et al. (2002) observed a significant correlation between lower P3b amplitude in an oddball task and higher numbing scores of the Clinician Administered PTSD Scale (CAPS; Blake et al., 1990, 1995). Additionally, Metzger et al. (1997a,b) suggested that the P3b amplitude in PTSD patients was confounded by their present level of anxiety as they reported a significant correlation between P3b amplitude and state anxiety score of the State and Trait Anxiety Inventory (STAI; Spielberger et al., 1983) in male Vietnam combat veterans with PTSD. However, the same research group (Metzger et al., 2002) found no association between P300 indices and clinical measures in female Vietnam nurse veterans with PTSD.

Moreover, no studies to date have evaluated neuroanatomical correlates of P300 abnormalities in PTSD patients, despite many independent publications of structural magnetic resonance imaging (MRI) abnormalities in PTSD such as those in anterior cingulate cortex (ACC) (Rauch et al., 2003; Yamasue et al., 2003) and hippocampus (Bremner et al., 1995; Gilbertson et al., 2002; Gurvits et al., 1996), brain regions thought to be associated with P300 generation (Halgren et al., 1980; Kiehl and Liddle, 2000; Mulert et al., 2004; Okada et al., 1983; Stevens et al., 2000).

The Tokyo subway sarin attack was perpetrated by terrorists belonging to a cult called "Aum Shinrikyo" in Japan on March 20, 1995. Sarin is a nerve gas and was used as a chemical weapon. As a result of the sarin attack, 12 victims died, 5500 people visited medical facilities, and 1046 people were admitted to 98 hospitals (Suzuki et al., 1995). Approximately 20 to 25% of the victims developed PTSD after this event (Kawana et al., 2001). Victims of the attack, both with and without PTSD, were recruited for the current study.

Consequently, the current study, for the first time in the literature, co-evaluated auditory P3b and MRI in never-treated, comorbid-free patients with PTSD following the Tokyo subway sarin attack. The victims of the same events who did not develop PTSD served as the control group. Our aims were: (1) to replicate P300 amplitude reduction in strictly sampled subjects with PTSD; (2) to assess a relationship between ERP indices and clinical symptoms; and importantly, (3) to seek a link between P300 amplitude abnormalities in PTSD and structural MRI abnormalities throughout the brain in PTSD using voxel-based morphometry (VBM) (Ashburner and Friston, 2000; Yamasue et al., 2003).

Methods

Subjects

A total of 47 subjects (24 males and 23 females, mean age = 42.1 [SD = 13.2]) was recruited from victims of the Tokyo subway sarin attack, who were treated in the emergency room for acute sarin intoxication with a follow up at St. Luke's International Hospital in Tokyo, Japan. Diagnostic interviews, ERP recordings, and MRI measurements (Yamasue et al., 2003) were performed between 2000 and 2001, 5–6 years after the incident. This sample largely overlapped with that of our previous near-infrared spectroscopy studies (Matsuo et al., 2003a,b). The participants completed the Impact of Event Scale-Revised (IES-R) (Weiss and Marmar, 1997; Japanese version: Asukai et al., 2002) and the STAI (Spielberger et al., 1983), and were interviewed by trained psychiatrists using the CAPS (Blake et al., 1990, 1995; Japanese version: Asukai and Nishizono-Maher, 1998). All subjects were also screened for the presence or absence of neuropsychiatric disorders by trained psychiatrists using the Mini-International Neuropsychiatric Interview (Sheehan et al., 1998). These interviews were performed on the same day as ERP recordings and MRI measurements.

Out of the 47 participants, 10 were diagnosed as having unequivocal PTSD related to the attack. Two of the 10 patients with PTSD who had psychiatric comorbidity ($N = 1$, current major depression; $N = 1$, current panic disorder with agoraphobia) were excluded from the final sample, since depression and panic disorder have themselves been reported to be associated with P300 abnormalities (Clark et al., 1996; Hansenne et al., 2000; Karaaslan et al., 2003; Pauli et al., 1997). Nineteen participants who fulfilled more than one, but not the full criteria of the three symptom clusters of PTSD in the CAPS (reexperiencing of the event, avoidance/numbing, and hypervigilance) (Mylle and Maes, 2004), were classified as having partial PTSD. On further analysis, these 19 victims were excluded from this study, since their inclusion would blur the difference in brain function between the PTSD subjects and controls. The remaining 18 victims had never had unequivocal or partial PTSD. However, 5 out of 18 were excluded for the following reasons: $N = 1$, a history of receiving hypnotics 2 years ago due to insomnia; $N = 4$, unsuccessful ERP measurements due to artifacts or technical problems.

Thus, the final set of subjects in this study included 8 (5 men and 3 women) victims with PTSD (2, current PTSD; 6, had history of PTSD) and 13 (8 men and 5 women) victims without PTSD who served as the control subjects. All were right-handed based on the Edinburgh Inventory (Oldfield, 1971); we determined the laterality index >0.8 as the cutoff for right-handedness. Age, gender, score of IES-R, STAI, and subject's and parental socioeconomic status (SES; Edinburgh Inventory; Hollingshead, 1965) were not significantly different between groups (Table 1). These 21 subjects had never received psychiatric treatment or medication before participating in this study. Moreover, none of the 21 subjects had a history of neurological illness, serious head trauma with any known cognitive consequences, or loss of consciousness for more than 5 min, or alcohol/substance abuse or dependence. None of the control subjects had a family history of axis I disorder in their first-degree relatives. Since acute sarin exposure modulates the cholinergic pathways (Khan et al., 2000), the concentrations of serum cholinesterase were evaluated to assess the severity of the acute sarin intoxication in the emergency room (Table 1). The ethical committee of the University of Tokyo Hospital approved of this study. After a complete explanation of the study to the subjects, written informed consent was obtained.

ERP recording

The subjects performed an oddball task to elicit P300 (P3b) in a soundproof room. They were presented with a series of auditory stimuli with a fixed interstimulus interval of 1500 ms. Eighty-five percent of the stimuli were tones of 1000 Hz, and the other 15% were tones of 2000 Hz. Stimuli were presented in a Bernoulli sequence. The subjects were instructed to keep their eyes closed

Table 1
Subject characteristics and clinical measures

Variable	Victims with PTSD (n = 8)		Victims without PTSD (n = 13)		Group comparison[a]		
	Mean	SD	Mean	SD	df	t Value	P
Age	46.6	14.8	47.6	11.5	19	0.17	0.87
Gender, male/female	5/3		8/5		...	...	0.66
Education, years	12.9	2.1	12.8	1.8	19	0.12	0.90
Socioeconomic status (SES)	2.3	0.5	2.5	0.7	16	0.53	0.60
Parental SES	3.0	1.1	3.0	0.7	16	0.0	1.0
Impact of event scale-revised (IES-R)	27.2	15.0	10.9	9.8	15	2.68	0.017
CAPS total (lifetime)	64.1	18.6	7.7	6.8	19	10.1	<0.001
CAPS total (present)	27.5	13.1	4.9	5.5	19	5.53	<0.001
STAI; trait anxiety score	48.0	10.3	40.2	7.0	18	2.03	0.057
STAI; state anxiety score	44.0	7.0	36.7	7.3	19	2.06	0.036
Concentrations of serum-cholinesterase, (IU/L)	110.8	29.2	150.3	20.5	10	−2.77	0.020

[a] Student's t tests were used, except for gender where Fisher's exact test was used.

throughout the tasks and to press a button with their right hand as quickly as possible upon hearing the infrequent high-pitch tones. The stimulus intensity was 75 dBSPL, and the tone duration was 50 ms, with a rise/fall time of 10 ms.

The scalp electroencephalogram (EEG) was recorded with Ag/Ag–Cl disc electrodes at Fp1, Fp2, F3, Fz, F4, T3, C3, Cz, C4, T4, T5, P3, Pz, P4, T6, and Oz according to the international 10–20 electrode system, referred to linked earlobes. Vertical and horizontal electrodes were placed below and at the outer canthus of the left eye. The sampling rate was 400 Hz, and the analog filter band-pass was 0.15–120 Hz. The analysis period was 640 ms, including a 40-ms prestimulus baseline. Trials contaminated by peak to peak potentials over 100 μV or accompanied by an EOG of over 75 μV were eliminated from the averaging. The responses to each stimulus with correct reactions were averaged separately. We recorded EEG until acquiring stable ERP data of 40 infrequent stimuli and 200 frequent stimuli. Finally, the averaged waveforms were digitally filtered with a cutoff frequency of 30 Hz. P300 were defined as the most positive peak between 250 and 500 ms poststimulus at Fz, T3, Cz, T4, and Pz.

Statistical analyses

Group differences in demographic, psychometric, and performance data (reaction time [RT] and % response accuracy) were examined using Student's t tests. Group differences in P300 amplitude and latency were evaluated using the repeated-measures analysis of variance (ANOVA) with group (victims with PTSD, those without PTSD) as the between-subject factor, and electrode site (Fz, T3, Cz, T4, and Pz) as the within-subject factor. Greenhouse–Geisser's correction was performed where appropriate and the associated epsilon and adjusted P values were reported.

Spearman's rho was calculated for correlations between P300 amplitudes at Cz or Pz and clinical measures, present and lifetime total and clusters B (reexperiencing), C (avoidance and numbing), and D (hyperarousal) scores of CAPS in the PTSD group. Here, we set the threshold for significance at P = 0.008 (Bonferroni correction: 0.05/6 correlations; two tailed). Correlational analyses were not performed for control subjects because of the very low scores of CAPS. Additionally, Spearman's correlations were also calculated between P300 amplitudes at Cz or Pz and IES-R scores, STAI scores, and concentrations of serum-cholinesterase which showed a significant difference between groups (Table 1), to test for their confounding effects for each group. Here, all correlations of $P < 0.05$ (two tailed) were reported in order not to underestimate the potential effects.

MRI acquisition

MRI data were obtained from 6 of 8 victims with PTSD using a 1.5-T scanner (General Electric Signa Horizon Lx version 8.2, GE Medical Systems, Milwaukee, WI, USA). The MR acquisition protocol has been described in detail elsewhere (Yamasue et al., 2003). Briefly, three-dimensional Fourier-transform spoiled gradient recalled acquisition with steady state was implemented. The repetition time was 35 ms, the echo time 7 ms with one repetition, the nutation angle 30°, the field of view 24 cm, and the matrix 256 × 256 (192) × 124. Voxel dimensions were 0.9375 × 0.9375 × 1.5 mm. A trained neuroradiologist (Ha.Ya. or O.A.) evaluated the MRI scans and found no gross abnormalities in any of the subjects.

MRI data analysis

The methods to analyze MRI data have been described in detail elsewhere (Yamasue et al., 2003). Briefly, image analysis was performed using ANALYZE PC 3.0 (Mayo Foundation, Rochester, MN, USA) and SPM 99 software (Wellcome Department of Cognitive Neurology, Institute of Neurology, London, UK) running in MATLAB 6.1 (Mathworks, Sherborn, MA). In ANALYZE, image data were resampled using an algorithm to make them isotropic, with the sides measuring 0.9375 mm and then stored. Resampled images were first spatially normalized into the standard space of Talairach and Tournoux (1988). Normalized images were then segmented into the gray matter, white matter, cerebrospinal fluid, and skull/scalp compartments using an automated and operator-independent process (Ashburner and Friston, 1997). The segmentation step also incorporates an image density nonuniformity correction (Ashburner and Friston, 2000) to address image density variations caused by different positions of cranial structures within the MRI head coil. The spatially normalized segments of gray and white matter were smoothed with a 12-mm full-width at half-maximum isotropic Gaussian kernel to accommodate individual variability in the sulcal and gyral anatomy. By smoothing the data, the partial volume effect was used to create a spectrum of gray or white matter intensities. Gray or white matter density is equivalent to the weighted average of the gray or white matter voxels located in the volume defined by the smoothing kernel. Since previous studies showed a fair correlation

between the regional gray or white matter density identified with VBM and their volumes measured by the conventional manual-tracing method (Kubicki et al., 2002; Richardson et al., 1997), the regional gray or white matter density can be considered to represent the local amount of gray or white matter.

Regional voxel-based analyses of the images were performed in SPM after covarying for global normalization, and these analyses can therefore be regarded as an analysis of covariance (ANCOVA) model (Friston et al., 1990). This removes global gray matter intensity for each subject, and normalizes the segmented brain images to the same total amount of gray matter while preserving regional differences in gray matter intensity. The P300 amplitudes at Pz were treated as the covariates of interest. To test hypotheses about regionally specific covariate effects, the estimates were compared using linear contrasts (positive or negative correlation) (Friston et al., 1995). The resulting set of voxel values for each contrast constituted a statistical parametric map of the t statistic (SPM(t)). The SPM(t) values were transformed to the normal distribution (SPM(z)) and thresholded at $P < 0.001$. The significance of each region was estimated by distributional approximations from the theory of random Gaussian fields. This characterization was in terms of the probability that the peak height observed could have occurred by chance over the entire volume analyzed. We adopted a very conservative threshold for significance (corrected $P < 0.05$) to avoid Type I errors. Since the correlational analysis was performed to examine the possible association between smaller ACC reported in our recent study (Yamasue et al., 2003) and reduced P300 amplitude, small volume correction was applied using the maxima obtained in our previous study ([−8, 12, 32]) as the center of a small volume (113 voxels).

Results

Performance data

Neither RT ($t = 0.72$, $df = 19$, $P = 0.48$), nor % response accuracy differed significantly between groups ($t = -1.19$, $df = 17$, $P = 0.25$) (Table 2).

P300 data

Groups differed significantly in P300 amplitude [main effect of group: $F(1,19) = 4.80$, $P = 0.041$), while the group-by-electrode interaction was not significant [$F(4,76) = 1.21$, $P = 0.32$, epsilon = 0.70] (Table 2, Fig. 1). For P300 latency, there was no significant main effect of group [$F(1,19) = 0.49$, $P = 0.49$] or group-by-electrode interaction [$F(4,76) = 0.35$, $P = 0.80$, epsilon = 0.80].

Table 2
Amplitude and latency of P300 indices

Variable	Victims with PTSD (n = 8)		Victims without PTSD (n = 13)	
	Mean	SD	Mean	SD
Reaction time (ms)	391	87	367	64
Response accuracy (%)	99.4	1.6	100.0	0.0
P3 amplitude at Pz (μV)	9.2	5.1	13.6	5.8
P3 latency at Pz (ms)	319	41	332	41

Correlation with clinical measures

In the PTSD group, there was a significantly negative correlation between present score of the cluster C of the CAPS and P300 amplitude at Pz (rho = −0.850, $N = 8$, uncorrected $P = 0.007$; corrected $P = 0.042$, two tailed). There were no significant correlations between P300 amplitudes and IES-R scores or between STAI scores and concentrations of serum-cholinesterase for either group (uncorrected Ps > 0.12).

Correlation with MRI measures

Within victims with PTSD, there was a trend-level positive correlation between the amplitude of P300 at Pz and the gray matter density in the left ACC gray matter (peak coordinate [x,y,z (mm)] = [−12,32,22], corrected $P = 0.077$, Z score = 4.08) (Fig. 2). This result suggests that reduced ACC gray matter volume may underlie auditory selective attention deficits as indexed by P300 in patients with PTSD. In the other regions, gray or white matter density was not significantly correlated with the amplitude of P300. In contrast, there was no voxel within left ACC correlated with the amplitude of P300 in victims without PTSD. Additionally, we did not find a significant correlation between P300 amplitude at Fz or Cz and voxel densities in victims with or without PTSD.

Discussion

We replicated a significant reduction in P300 amplitude in the oddball task in PTSD patients who were victims of Tokyo subway sarin attack compared with those victims who did not develop PTSD. We found a significant correlation between P300 amplitude and avoidance/numbing cluster score of the CAPS. Furthermore, lower P300 amplitudes showed a trend toward significant correlation with smaller gray matter voxel densities of ACC in victims with PTSD, whereas such an association was not present in victims without PTSD. While the P300 has multiple generators in humans, a smaller ACC volume in the individuals with PTSD may be proportional to lower functioning of ACC which is one of the generators of the P300, thus resulting in a tighter structure–function relationship in the PTSD group. To our knowledge, this is the first report that links P300 electrophysiological deficits to underlying neuroanatomical abnormalities in PTSD that had been only independently evaluated in the previous literature.

The strengths of our study include the common exposure to the same traumatic event of both the control and PTSD groups, and the strict exclusion criteria for any condition that may affect P300 indices such as prior psychotropic treatment, history of alcohol and substance misuse, and psychiatric comorbidity, which have not been always controlled in previous literature. Tochigi et al. (2002) reported a significant reduction of the serum cholinesterase concentration in victims with PTSD caused by Tokyo subway sarin attack, and suggested that the reduction of the serum cholinesterase concentration might partly reflect the effect of sarin intoxication. In addition, Metzger et al. (1997a,b) suggested that the P3b amplitude in PTSD patients was associated with their state anxiety score of the STAI. In our study, however, the lower P300 amplitude in the PTSD group was not likely to be solely a consequence of the group difference

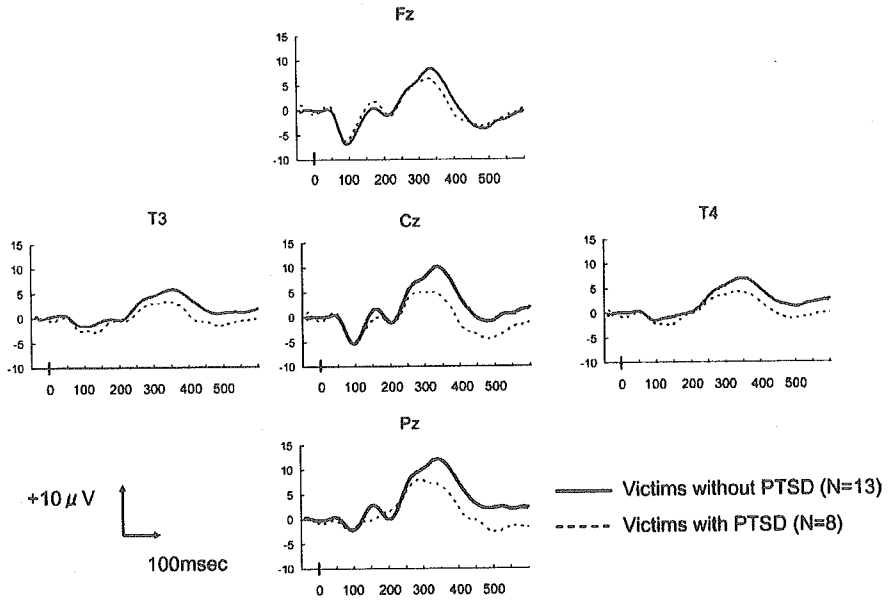

Fig. 1. P300 waveforms in victims with and without PTSD. Grand mean ERPs in response to target tones at five electrodes averaged across subjects. Solid lines represent waveforms for victims without PTSD; dashed lines represent those with PTSD. Horizontal axis is in milliseconds. Vertical axis is in microvolt; positivity is denoted by upward direction.

observed in concentrations of serum cholinesterase just after poisoning or levels of state and trait anxiety, since there were no significant correlations between P300 amplitude and these clinical measures in either group.

To our best knowledge, this study is the first to explore the anatomical correlates of P300 reduction observed in patients with PTSD. We have previously found a significant reduction of ACC gray matter volume in the largely overlapped sample exposed to the

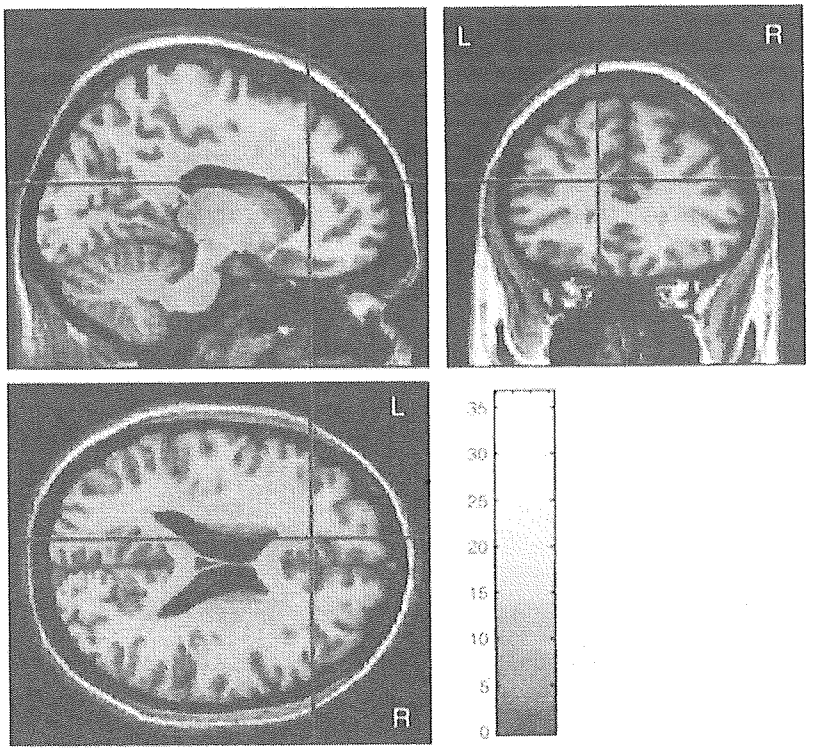

Fig. 2. Brain regions correlated with P300 amplitude in victims with PTSD. Voxel densities in the anterior cingulate cortex gray matter showed a trend toward significant association with P300 amplitudes at Pz in victims with PTSD (corrected $P = 0.077$). These voxels were highlighted and rendered onto orthogonal slices of the normal template MR images.

same event (Yamasue et al., 2003). The P300 has been thought to have multiple generators including superior temporal gyrus (e.g., McCarley et al., 1993, 2002), hippocampus (Halgren et al., 1980; Okada et al., 1983), lateral prefrontal cortex (e.g., Kirino et al., 2000; Knight, 1984), and ACC (Ardekani et al., 2002; Dien et al., 2003; Kiehl and Liddle, 2000; Woldorff et al., 1999). The results of the present study suggest that structural abnormalities of the ACC in PTSD may contribute to functional abnormalities of controlled attention as indexed by P300. Our results are also in line with a growing body of functional (Bremner et al., 1999a,b; Shin et al., 1999, 2001) and structural (Rauch et al., 2003; Yamasue et al., 2003) neuroimaging work that proposes an important role of ACC in the pathophysiology of PTSD. Matsuo et al. (2003b), using a largely overlapped sample of victims of the Tokyo subway sarin attack, showed a reduced activation of lateral prefrontal cortex during a verbal fluency task by means of near-infrared spectroscopy in patients with PTSD. Since they found a significant positive correlation between smaller total hemoglobin increases and lower neuropsychological scores on attention and concentration, they interpreted the observed lateral prefrontal dysfunction as a secondary phenomenon to reduced attentional capacity in patients with PTSD. Our findings of reduced P300 as an indicator for capacity of attentional allocation may provide a support for this interpretation.

In the present study, we found a significant negative correlation between P300 amplitude and avoidance/numbing cluster scores of the CAPS. This is compatible with the results from Felmingham et al. (2002) study which found a significant correlation between P300 amplitude in an oddball task and numbing scores of the CAPS. Thus, our study further suggests that electrophysiological abnormalities of stimulus evaluation may at least partially underlie the clinical symptoms of PTSD. ACC may be involved in selective attention and inhibitory control of cognition and emotion (Bush et al., 2000; Carter et al., 1997). P300 is also believed to be an index of selective attention and context updating (Donchin and Coles, 1988; Picton, 1992; Polich and Kok, 1995). The relationship between P300 amplitude and avoidance/numbing symptom may thus indicate that functional abnormalities in the ACC may underlie the basis for specific symptoms in PTSD.

The design of this cross-sectional study cannot directly address the etiology of the P300 reduction, i.e., whether it is a vulnerability marker or a consequence of the chronic effect of stress. However, the relationship with the present CAPS score does not necessarily mean that the P300 reduction found in our study represents a state marker. Our previous study (Yamasue et al., 2003) also reported a correlation between the smaller ACC volume and severer present symptoms in the PTSD group. In addition, a twin study (Gilbertson et al., 2002) reported that the present PTSD severity in the combat-exposed PTSD subjects was negatively correlated with the hippocampal volume of both the patients and their unexposed co-twins. Furthermore, they also reported that both PTSD subjects and their unexposed co-twins had significantly smaller hippocampal volume than combat-exposed non-PTSD subjects and their unexposed co-twins. They concluded that a smaller hippocampus constitutes a vulnerability marker for the development of PTSD in trauma-exposed individuals. Therefore, we speculate that our findings may also serve as a vulnerability marker that could predict the severity of PTSD symptoms in the chronic status.

Methodological considerations of our study need to be mentioned. First, the strict exclusion criteria applied to this valuable sample resulted in a small final sample size, especially for the correlational analysis between P300 and MRI. However, we examined the robustness of our results by performing a resampling procedure, where PTSD and control subjects were randomly assigned to two groups and the group difference in P300 amplitude was computed for 50 times. As a result, none of the comparisons reached significance [$F(1,19) = 0.001$–4.26; $P = 0.053$–0.98]. We also checked the likelihood of the P300-ACC correlation by using the resampling procedure, where we calculated the correlation between P300 amplitude and peak voxel density of the ACC in randomly assigned PTSD group for 50 times. Again, none of the correlations reached significance ($R = -0.486$–0.714; $P = 0.11$–0.96). Second, the significance level of neuroanatomical correlates of P300 abnormality was marginal (corrected $P = 0.077$), since we adopted a very conservative threshold for significance to avoid Type I errors. However, it has been suggested that the SPM software's correction for multiple comparisons (originally designed to analyze functional imaging data) may be too strict when applied to the analysis of structural data (Salgado-Pineda et al., 2003), where the authors proposed that regions with uncorrected $P < 0.001$ should be regarded to be significant. Future studies with a larger sample size will be necessary to reach a definitive conclusion. Third, the interpretation of the results of correlational analysis needs to be done with caution, since the correlation cannot lead to a definitive conclusion about the cause–effect relationship. Therefore, there remains a possibility that our results may indicate an indirect link between ACC abnormality and abnormal P300 generation and an undetected, third effect may contribute to both abnormalities. Finally, we excluded the partial PTSD group because we thought that their inclusion would blur the difference in brain function between the PTSD subjects and controls. In fact, P300 amplitude for the partial PTSD group ($N = 11$ after applying exclusion criteria for confounding status; mean amplitude at Pz, 13.5 μV) was comparable with that for the control group (mean, 13.6 μV), and they were not statistically different ($P = 0.98$). The partial PTSD group and the PTSD group did not also differ in P300 amplitude ($P = 0.25$). There was no significant correlation between P300 amplitude and the scores of the CAPS. Moreover, the correlation between the P300 amplitude and the ACC morphology in the victims with partial PTSD symptoms ($N = 9$) were not statistically significant.

In conclusion, we replicated lower P300 amplitudes that were significantly associated with higher avoidance/numbing scores in patients with PTSD due to terrorism. More importantly, in the PTSD group only, the P300 amplitude showed a trend toward positive correlation with gray matter volume of ACC. These results provide the first evidence that electrophysiological deficits in controlled attention in PTSD are linked to underlying brain morphological abnormalities.

Acknowledgments

This study was performed through Special Coordination Funds for Promoting Science and Technology from the Ministry of Education, Culture, Sports, Science and Technology, the Japanese Government. The authors gratefully thank Dr. Shin-ichi Ishimatsu (St. Luke's International Hospital, Emergency Unit) who helped us to enroll the subjects, Drs. Hiroshi Matsuda and Takashi Ohnishi for their technical advice on voxel-based morphometry, and Dr.

Mark Rogers for his helpful comments and English editing of the manuscript.

References

Ardekani, B.A., Choi, S.J., Hossein-Zadeh, G.A., Porjesz, B., Tanabe, J.L., Lim, K.O., et al., 2002. Functional magnetic resonance imaging of brain activity in the visual oddball task. Brain Res., Cogn. Brain Res. 14, 347–356.

Ashburner, J., Friston, K., 1997. Multimodal image coregistration and partitioning—a unified framework. NeuroImage 6, 209–217.

Ashburner, J., Friston, K.J., 2000. Voxel-based morphometry—the methods. NeuroImage 11, 805–821.

Asukai, N., Nishizono-Maher, A., 1998. The Japanese Version of Clinician-Administered PTSD Scale. Tokyo Institute of Psychiatry, Tokyo.

Asukai, N., Kato, H., Kawamura, N., Kim, Y., Yamamoto, K., Kishimoto, J., et al., 2002. Reliability and validity of the Japanese-language version of the impact of event scale-revised (IES-R-J): four studies of different traumatic events. J. Nerv. Ment. Dis. 190, 175–182.

Blake, D.D., Weathers, F.W., Nagy, L.M., Kaloupek, D.G., Klauminzer, G., Charney, D.S., et al., 1990. A clinician rating scale for assessing current and lifetime PTSD: the CAPS-1. Behav. Ther. 13, 187–188.

Blake, D.D., Weathers, F.W., Nagy, L.M., Kaloupek, D.G., Gusman, F.D., Charney, D.S., et al., 1995. The development of a clinician-administered PTSD scale. J. Trauma. Stress 8, 75–90.

Bremner, J.D., Randall, P., Scott, T.M., Bronen, R.A., Seibyl, J.P., Southwick, S.M., et al., 1995. MRI-based measurement of hippocampal volume in patients with combat-related posttraumatic stress disorder. Am. J. Psychiatry 152, 973–981.

Bremner, J.D., Narayan, M., Staib, L.H., Southwick, S.M., McGlashan, T., Charney, D.S., 1999a. Neural correlates of memories of childhood sexual abuse in women with and without posttraumatic stress disorder. Am. J. Psychiatry 156, 1787–1795.

Bremner, J.D., Staib, L.H., Kaloupek, D., Southwick, S.M., Soufer, R., Charney, D.S., 1999b. Neural correlates of exposure to traumatic pictures and sound in Vietnam combat veterans with and without posttraumatic stress disorder: a positron emission tomography study. Biol. Psychiatry 45, 806–816.

Bush, G., Luu, P., Posner, M.I., 2000. Cognitive and emotional influences in anterior cingulate cortex. Trends Cogn. Sci. 4, 215–222.

Carter, C.S., Mintun, M., Nichols, T., Cohen, J.D., 1997. Anterior cingulate gyrus dysfunction and selective attention deficits in schizophrenia: [15O]H2O PET study during single-trial Stroop task performance. Am. J. Psychiatry 154, 1670–1675.

Charles, G., Hansenne, M., Ansseau, M., Pitchot, W., Machowski, R., Schittecatte, M., et al., 1995. P300 in posttraumatic stress disorder. Neuropsychobiology 32, 72–74.

Clark, C.R., McFarlane, A.C., Weber, D.L., Battersby, M., 1996. Enlarged frontal P300 to stimulus change in panic disorder. Biol. Psychiatry 39, 845–856.

Comerchero, M.D., Polich, J., 1999. P3a and P3b from typical auditory and visual stimuli. Clin. Neurophysiol. 110, 24–30.

Dien, J., Spencer, K.M., Donchin, E., 2003. Localization of the event-related potential novelty response as defined by principal components analysis. Brain Res., Cogn. Brain Res. 17, 637–650.

Donchin, E., Coles, M.G.H., 1988. Is the P300 component a manifestation of context updating? Behav. Brain Sci. 11, 357–374.

Felmingham, K.L., Bryant, R.A., Kendall, C., Gordon, E., 2002. Event-related potential dysfunction in posttraumatic stress disorder: the role of numbing. Psychiatry Res. 109, 171–179.

Ford, J.M., Roth, W.T., Kospell, B.S., 1976. Attention effects on auditory evoked potentials to infrequent events. Biol. Psychiatry 4, 65–77.

Friston, K.J., Frith, C.D., Liddle, P.F., Dolan, R.J., Lammertsma, A.A., Frackowiak, R.S., 1990. The relationship between global and local changes in PET scans. J. Cereb. Blood Flow Metab. 10, 458–466.

Friston, K.J., Holms, A.P., Worsley, K.J., Poline, J.B., Frith, C.D., Frackowiak, R.S., 1995. Statistical parametric maps in functional imaging. Hum. Brain Mapp. 2, 189–210.

Gilbertson, M.W., Shenton, M.E., Ciszewski, A., Kasai, K., Lasko, N.B., Orr, S.P., et al., 2002. Smaller hippocampal volume predicts pathologic vulnerability to psychological trauma. Nat. Neurosci. 5, 1242–1247.

Gurvits, T.V., Shenton, M.E., Hokama, H., Ohta, H., Lasko, N.B., Gilbertson, M.W., et al., 1996. Magnetic resonance imaging study of hippocampal volume in chronic, combat-related posttraumatic stress disorder. Biol. Psychiatry 40, 1091–1099.

Halgren, E., Squires, N.K., Wilson, C.L., Rohrbaugh, J.W., Babb, T.L., Crandall, P.H., 1980. Endogenous potentials generated in the human hippocampal formation and amygdale by infrequent events. Science 210, 803–805.

Hansenne, M., Pitchot, W., Pinto, E., Reggers, J., Papart, P., Ansseau, M., 2000. P300 event-related brain potential and personality in depression. Eur. Psychiatry 15, 370–377.

Hollingshead, A.B., 1965. Two-Factor Index of Social Position. Yale University Press, New Haven, CT.

Karaaslan, F., Gonul, A.S., Oguz, A., Erdinc, E., Esel, E., 2003. P300 changes in major depressive disorders with and without psychotic features. J. Affect Disord. 73, 283–287.

Katayama, J., Polich, J., 1998. Stimulus context determines P3a and P3b. Psychophysiology 35, 23–33.

Kawana, N., Ishimatsu, S., Kanda, K., 2001. Psycho-physiological effects of the terrorist sarin attack on the Tokyo subway system. Mil. Med. 166, 23–26.

Khan, W.A., Dechkovskaia, A.M., Herrick, E.A., Jones, K.H., Abou-Donia, M.B., 2000. Acute sarin exposure causes differential regulation of choline acetyltransferase, acetylcholinesterase, and acetylcholine receptors in the central nervous system of the rat. Toxicol. Sci. 57, 112–120.

Kiehl, K.A., Liddle, P.F., 2000. An event-related functional magnetic resonance imaging study of an auditory oddball task in schizophrenia. Schizophr. Res. 48, 159–171.

Kimble, M., Kaloupek, D., Kaufman, M., Deldin, P., 2000. Stimulus novelty differentially affects attentional allocation in PTSD. Biol. Psychiatry 47, 880–890.

Kirino, E., Belger, A., Goldman-Rakic, P., McCarthy, G., 2000. Prefrontal activation evoked by infrequent target and novel stimuli in a visual target detection task: an event-related functional magnetic resonance imaging study. J. Neurosci. 20, 6612–6618.

Knight, R.T., 1984. Decreased response to novel stimuli after prefrontal lesions in man. Electroencephalogr. Clin. Neurophysiol. 59, 9–20.

Kubicki, M., Shenton, M.E., Salisbury, D.F., Hirayasu, Y., Kasai, K., Kikinis, R., et al., 2002. Voxel-based morphometric analysis of gray matter in first episode schizophrenia. NeuroImage 17, 1711–1719.

Matsuo, K., Kato, T., Taneichi, K., Matsumoto, A., Otani, T., Hamamoto, T., et al., 2003a. Activation of the prefrontal cortex to trauma-related stimuli measured by near-infrared spectroscopy in posttraumatic stress disorder due to terrorism. Psychophysiology 40, 492–500.

Matsuo, K., Taneichi, K., Matsumoto, A., Otani, T., Yamasue, H., Sakano, Y., et al., 2003b. Hypoactivation of the prefrontal cortex during verbal fluency test in PTSD: a near-infrared spectroscopy study. Psychiatry Res. 124, 1–10.

McCarley, R.W., Shenton, M.E., O'Donnell, B.F., Faux, S.F., Kikinis, R., Nestor, P.G., et al., 1993. Auditory P300 abnormalities and left posterior superior temporal gyrus volume reduction in schizophrenia. Arch. Gen. Psychiatry 50, 190–197.

McCarley, R.W., Salisbury, D.F., Hirayasu, Y., Yurgelun-Todd, D.A., Tohen, M., Zarate, C., et al., 2002. Association between smaller left posterior superior temporal gyrus volume on magnetic resonance imaging and smaller left temporal P300 amplitude in first-episode schizophrenia. Arch. Gen. Psychiatry 59, 321–331.

McFarlane, A.C., Weber, D.L., Clark, C.R., 1993. Abnormal stimulus processing in posttraumatic stress disorder. Biol. Psychiatry 34, 311–320.

Metzger, L.J., Orr, S.P., Lasko, N.B., McNally, R.J., Pitman, R.K., 1997a.

Seeking the source of emotional Stroop interference effects in PTSD: a study of P3s to traumatic words. Integr. Physiol. Behav. Sci. 32, 43–51.
Metzger, L.J., Orr, S.P., Lasko, N.B., Pitman, R.K., 1997b. Auditory event-related potentials to tone stimuli in combat-related posttraumatic stress disorder. Biol. Psychiatry 42, 1006–1015.
Metzger, L.J., Carson, M.A., Paulus, L.A., Lasko, N.B., Paige, S.R., Pitman, R.K., et al., 2002. Event-related potentials to auditory stimuli in female Vietnam nurse veterans with posttraumatic stress disorder. Psychophysiology 39, 49–63.
Mulert, C., Jager, L., Schmitt, R., Bussfeld, P., Pogarell, O., Moller, H.J., et al., 2004. Integration of fMRI and simultaneous EEG: towards a comprehensive understanding of localization and time-course of brain activity in target detection. NeuroImage 22, 83–94.
Mylle, J., Maes, M., 2004. Partial posttraumatic stress disorder revisited. J. Affective Disord. 78, 37–48.
Neylan, T.C., Jasiukaitis, P.A., Lenoci, M., Scott, J.C., Metzler, T.J., Weiss, D.S., et al., 2003. Temporal instability of auditory and visual event-related potentials in posttraumatic stress disorder. Biol. Psychiatry 53, 216–225.
Okada, Y.C., Kaufman, L., Williamson, S.J., 1983. The hippocampal formation as a source of the slow endogenous potentials. Electroencephalogr. Clin. Neurophysiol. 55, 417–426.
Oldfield, R.C., 1971. The assessment and analysis of handedness: the Edinburgh inventory. Neuropsychologia 9, 97–113.
Pauli, P., Dengler, W., Wiedemann, G., Montoya, P., Flor, H., Birbaumer, N., et al., 1997. Behavioral and neurophysiological evidence for altered processing of anxiety-related words in panic disorder. J. Abnorm. Psychology 106, 213–220.
Picton, T.W., 1992. The P300 wave of the human event-related potential. J. Clin. Neurophysiol. 9, 456–479.
Polich, J., Kok, A., 1995. Cognitive and biological determinants of P300: an integrated review. Biol. Psychology 41, 103–146.
Rauch, S.L., Shin, L.M., Segal, E., Pitman, R.K., Carson, M.A., McMullin, K., et al., 2003. Selectively reduced regional cortical volumes in post-traumatic stress disorder. NeuroReport 14, 913–916.
Richardson, M.P., Friston, K.J., Sisodiya, S.M., Koepp, M.J., Ashburner, J., Free, S.L., et al., 1997. Cortical grey matter and benzodiazepine receptors in malformations of cortical development. A voxel-based comparison of structural and functional imaging data. Brain 120, 1961–1973.
Salgado-Pineda, P., Baeza, I., Perez-Gomez, M., Vendrell, P., Junque, C., Bargallo, N., et al., 2003. Sustained attention impairment correlates to gray matter decreases in first episode neuroleptic-naive schizophrenic patients. NeuroImage 19, 365–375.
Sheehan, D.V., Lecrubier, Y., Sheehan, K.H., Amorim, P., Janavs, J., Weiller, E., et al., 1998. The Mini-International Neuropsychiatric Interview (M.I.N.I.): the development and validation of a structured diagnostic psychiatric interview for DSM-IV and ICD-10. J. Clin. Psychiatry 59, 22–33.
Shin, L.M., McNally, R.J., Kosslyn, S.M., Thompson, W.L., Rauch, S.L., Alpert, N.M., et al., 1999. Regional cerebral blood flow during script-driven imagery in childhood sexual abuse-related PTSD: a PET investigation. Am. J. Psychiatry 156, 575–584.
Shin, L.M., Whalen, P.J., Pitman, R.K., Bush, G., Macklin, M.L., Lasko, N.B., et al., 2001. An fMRI study of anterior cingulate function in posttraumatic stress disorder. Biol. Psychiatry 50, 932–942.
Spielberger, C.D., Gorsuch, R.L., Lushene, R.E., Vagg, P.R., Jacobs, G.A., 1983. STAI: Manual for the State-Trait Anxiety Inventory. Consulting Psychologists Press, Palo Alto, CA.
Stevens, A.A., Skudlarski, P., Gatenby, J.C., Gore, J.C., 2000. Event-related fMRI of auditory and visual oddball tasks. Magn. Reson. Imaging 18, 495–502.
Suzuki, T., Morita, H., Ono, K., Maekawa, K., Nagai, R., Yazaki, Y., 1995. Sarin poisoning in Tokyo subway. Lancet 345, 980–981.
Talairach, J., Tournoux, P., 1988. Co-Planar Stereotaxic Atlas of the Human Brain. George Thieme, Stuttgart.
Tochigi, M., Umekage, T., Otani, T., Kato, T., Iwanami, A., Asukai, N., et al., 2002. Serum cholesterol, uric acid and cholinesterase in victims of the Tokyo subway sarin poisoning: a relation with post-traumatic stress disorder. Neurosci. Res. 44, 267–272.
Weiss, D.S., Marmar, C.R., 1997. The impact of event scale-revised. In: Wilson, J.P., Keane, T.M. (Eds.), Assessing Psychological Trauma and PTSD. The Guilford Press, New York, pp. 399–411.
Woldorff, M.G., Matzke, M., Zamarripa, F., Fox, P.T., 1999. Hemodynamic and electrophysiological study of the role of the anterior cingulate in target-related processing and selection for action. Hum. Brain Mapp. 8, 121–127.
Yamasue, H., Kasai, K., Iwanami, A., Ohtani, T., Yamada, H., Abe, O., et al., 2003. Voxel-based analysis of MRI reveals anterior cingulate gray-matter volume reduction in posttraumatic stress disorder due to terrorism. Proc. Natl. Acad. Sci. U. S. A. 100, 9039–9043.

Tissue specificity of methylation and expression of human genes coding for neuropeptides and their receptors, and of a human endogenous retrovirus K family

Hong-mei Shen,[1] Akifumi Nakamura,[1,2] Jun Sugimoto,[1] Noboru Sakumoto,[2] Takaya Oda,[1] Yoshihiro Jinno,[1] Yuji Okazaki[3]

[1]Department of Molecular Biology and [2]Department of Neuropsychiatry,
Ryukyu University School of Medicine, Okinawa, Japan
[3]Department of Neuropsychiatry, Mie University School of Medicine, Mie, Japan

Correspondence: Y Jinno, Department of Molecular Biology, Ryukyu University School of Medicine, 207 Nishihara, Okinawa 903-0215, Japan
Fax: +81-98-895-1438; Tel: +81-98-895-3331; E-mail: sirius@med.u-ryukyu.ac.jp

Abstract The purpose of the present study was to understand the tissue specificity of DNA methylation and the relationship between methylation and expression of genes with essential roles in neurodevelopment and brain function. We chose dopamine receptor genes (*DRD1* and *DRD2*), *NCAM*, and *COMT* as examples of genes with CpG islands around the promoter region, and serotonin receptor genes (*HTR2A* and *HTR3A*), *HCRT*, and *DRD3* as genes without CpG islands. Methylation states were investigated in fetal brain, fetal liver, placenta, and adult peripheral leukocytes from three individuals by Southern blot and bisulfite-modified DNA sequencing. A repetitive sequence, human endogenous retrovirus (HERV)-K was also examined. All genes examined were almost completely unmethylated in brains. The genes with CpG islands were unmethylated regardless of their expression state. In contrast, genes without CpG islands showed various methylation patterns, which did not necessarily reflect the transcriptional activity of the genes. Most HERV-K loci were methylated, but some loci showed relatively low methylation in the placenta and liver. Interestingly, we found inter-individual differences in methylation levels in *HTR2A* and *HCRT* in the placenta and in some loci of HERV-K in the placenta and liver. The sample with the lowest methylation levels in the two unique genes showed higher methylation of HERV-K loci than the other samples. These results provide detailed information about the methylation states of the genes analyzed and evidence for inter-individual variations in methylation in both unique and repetitive sequences.

Key words: tissue specificity; DNA methylation; gene expression; dopamine and serotonin receptors; human endogenous retrovirus

Introduction

Epigenetic modifications are involved in a wide range of normal and pathological cellular phenomena (Jones and Laird 1999; Jaenisch and Bird 2003). Cytosine methylation in CpG and some CpNpG sequences is the sole epigenetic modification of DNA with known biological functions. One of these functions is gene regulation through the construction of heterochromatin (Razin 1998). Unusual hypermethylation has often been observed in tumors in the promoter regions of tumor suppressor genes (Jones and Laird 1999).

Aberrant epigenetic modifications occur not only in somatic cells, resulting in tumors, but also in some inherited diseases (Bickmore and van der Maarel 2003). Mental dysfunction is a major symptom in most inherited diseases with aberrations in epigenetic modifications. The neurodevelopmental disorder Rett syndrome is caused by mutations in a methyl-CpG-binding protein, MeCP2, and the characteristic clinical features partially resemble those observed in autism and schizophrenia (Robertson and Wolffe 2000; Shahbazian and Zoghbi 2002). Rett syndrome is a typical example of the implications of epigenetic modifications such as DNA methylation, and suggests that accurate fine-tuning of gene expression by epigenetic mechanisms is essential for normal brain function.

Studies on the role of DNA methylation in the pathogenesis of psychiatric disorders have increased in recent years but are still few in number, which may be due to the unique features of DNA methylation as well as the technical challenges involved in correlating methylation with particular pathologies. DNA methylation undergoes a genome-wide erasure and re-establishment during embryogenesis and shows tissue-specific patterns, as does gene expression (Hsieh 2000). It is evident that two major psychiatric disorders, schizophrenia and bipolar disorder, are inherited illnesses, and it is also true that both disorders are greatly influenced by environmental conditions (Abdolmaleky et al. 2005). Although seemingly paradoxical, DNA methylation could explain both the ambiguous inheritance and the roles of environmental factors in the etiology of these disorders. There is increasing evidence that some epigenetic signals may exhibit partial meiotic stability and can be transmitted from one generation to the next (Roemer et al. 1997; Morgan et al. 1999; Sutherland et al. 2000; Rakyan et al. 2002). Similarly, mitotic transmission of DNA methylation patterns demonstrates partial stability, but such patterns can be changed by hormones, nutritional factors, aging, or stochastic events in the cell (Wolff et al. 1998;

Ahuja and Issa 2000; Thomassin et al. 2001).

In the present study, we examined the DNA methylation status of eight genes that are actively expressed in the brain: the dopamine receptors *DRD1*, *DRD2*, and *DRD3*, catechol-O-methyltransferase (*COMT*), neural cell adhesion molecule (*NCAM*), the 5-hydroxytryptamine receptors *HTR2A* and *HTR3A*, and hypocretin (*HCRT*; also called orexin). *DRD1, DRD2, COMT,* and *NCAM* harbor CpG islands around the promoter regions and the other four genes do not. In addition to these eight single copy genes, we also examined methylation states in the 5' long terminal repeat (LTR) of the human endogenous retrovirus (HERV)-K family in order to compare patterns between unique sequences and repetitive sequences, as well as to examine possible inter-individual differences.

Materials and methods

DNA and RNA

In the present study, we used DNA and RNA extracted from human fetal whole brains, fetal livers, placentas, and from peripheral blood leukocytes (PBL) of healthy volunteers. We prepared DNA using the standard proteinase K/phenol method (Sambrook et al. 1989). RNA from tissues other than PBL was extracted by the guanidine/CsCl method (Sambrook et al. 1989). RNA from PBL was isolated using ISOGEN (Nippon Gene, Japan) according to the manufacturer's instructions. DNA and RNA from fetal tissues and placentas were all from samples obtained in 1997. The fetuses (and placentas) were artificially aborted at 16 (Sample a), 19 (Sample b), and 21 (Sample c) weeks of gestation. Detailed information on the fetuses was not available.

Methylation analyses

We examined the methylation states of the eight single copy genes by Southern blot hybridization and using the sodium bisulfite-modified DNA sequencing method. HERV-K methylation was examined by Southern blot hybridization alone. Using the Grail 1.3 program (http://compbio.ornl.gov/Grail-1.3/), we confirmed that the sequences to be analyzed satisfied the established definition of a CpG island. DNA was first digested

with appropriate non-methylsensitive restriction enzymes to yield a distinct band(s) in the methylation analysis by Southern blot hybridization. The restriction digests were then digested with methylsensitive restriction enzymes (10 units per μg DNA), separated on 0.8% agarose gels, and transferred to Hybond-N^+ membrane (Amersham Biosciences, Piscataway, NJ). Probes for the Southern blot hybridization were amplified by PCR, cloned into the pGEM-T easy vector (Promega, Madison, WI), and confirmed by sequencing. Probe DNA was labeled with [α-^{32}P]dCTP using a Megaprime DNA Labeling kit (Amersham Biosciences). Primer sequences and temperatures for the final wash of the hybridized membranes are shown in Table 1. The blots were hybridized in 6xSSC / 0.5% SDS at 65°C overnight and were sequentially washed in 2xSSC / 0.1% SDS at 55°C and in 0.1xSSC / 0.1% SDS at the appropriate temperatures (Table 1).

Sodium bisulfite treatment was carried out as described (Grunau et al. 2001), with minor modifications. The bisulfite-treated DNA was amplified by PCR using the following conditions: denaturation at 94°C for 3 min, followed by 35 cycles of 94°C for 1 min, annealing temperature (see Table 2) for 1 min, 72°C for 1 min, and a final elongation at 72°C for 5 min with a GeneAmp PCR System 9600 (Applied Biosystems, Foster City, CA). Nested PCR was performed for 25 cycles. The primer sequences and sizes and positions of the regions analyzed are shown in Table 2. The primer sequences were designed using a program for predicting modified sequences (Singal and Grimes, 2001). The PCR products were cloned into the pGEM-T easy vector (Promega), and 10 clones each were sequenced using a BigDye sequencing kit (Applied Biosystems). In the case of the CpG island genes, we performed the methylation analysis using the bisulfite method only for fetal brain and adult PBL from one fetus and one person, respectively.

Reverse transcription-PCR

RNA used for RT-PCR was pre-treated twice with 10 to 30 U RNase-free DNase I (Roche, Mannheim, Germany) for 40 min at 37°C. DNase I-treated total RNA (5 μg) was reverse-transcribed with random primers and the M-MLV reverse transcriptase (Invitrogen, La Jolla, CA) for 1 h at 37°C in a 20 μl reaction mix. The reverse transcription products were diluted 6- to 25-fold and 2 μl used for PCR (18-36 cycles) in a total volume of 20 μl. The PCR products were separated by electrophoresis using a 6.0% polyacrylamide gel. The intensity of the PCR products was measured using Science